

Material of oxo-peroxo-molybdenum (VI) complex involving 4-Furoyl-3-methyl-1-phenyl-2-pyrazoline-5-one: experimental cum theoretical observations

Abstract

We report here the experimental and theoretical investigation of the bis(4-furoyl-3-methyl-1-phenyl-2-pyrazolin-5-one)oxoperoxomolybdenum(VI) complex molecule. It was prepared by the reaction of (2:1) 4-furoyl-3-methyl-1-phenyl-2-pyrazolin-5-one and $[\text{MoO}(\text{O})_2]^{2+}$ in an aqueous ethanol medium. Characterization was performed by elemental analysis, molar conductivity, magnetic measurements, electrochemical analysis, and infrared and electronic spectral studies. Theoretical validation was performed by density functional theory calculations using B3LYP as the LANL2DZ function. The molecular geometry results show a distorted pseudo-pentagonal bipyramidal geometry together with the O_2 coordination mode around the Mo(VI) center. The FMO energies allow the determination of the atomic and molecular parameters and also represent the charge transfer across the molecule.

Keywords: oxidoperoxidomolybdenum, electrochemistry, density functional theory, frontier molecular orbitals, molecular electrostatic potential surfaces

Volume 7 Issue 2 - 2023

PK Vishwakarma, PS Jaget, MK Parte, VS Lodhi, RC Maurya

Department of PG Studies and Research in Chemistry and Pharmacy, Rani Durgavati Vishwavidyalaya, India

Correspondence: PK Vishwakarma, Department of PG Studies and Research in Chemistry and Pharmacy, Rani Durgavati Vishwavidyalaya, Jabalpur, M.P, India, Tel +917974714084, Email pkvchemrduini@gmail.com

Received: April 13, 2023 | Published: May 15, 2023

Introduction

Acylpyrazolones were previously explored by Jensen¹ and have been used for numerous applications, such as pigments for dyes, metal extractants from acidic solutions, and also as sequestering agents for environmentally harmful metal ions such as lead and cadmium.² These ligands have played an important role in the development of coordination compounds with a wide range of metal complexes that have applications in numerous fields, from new materials to catalysts, as precursors for CVD in the microelectronics industry, and as potent antitumor agents.³ Pyrazolones are reported to have potent antibacterial, antifungal, antihistaminic, analgesic, antipyretic, anti-inflammatory, and antirheumatic activities. In addition, antidiabetic⁴ and anticancer⁵ properties have been demonstrated.

Molybdenum (Mo) is the only second-tier transition metal required by most living organisms and is almost universally distributed in biology.⁶ Molybdenum is an important trace element involved in the structure of certain enzymes and catalyzes redox reactions.⁷ Certain molybdenum compounds are used to treat Wilson's disease,⁸ to lower blood sugar levels,⁹ and as anticancer drugs.¹⁰ The peroxo and proxy complexes of transition metals have played an essential role in the epoxidation of alkene substrates to their epoxy products for some time.

Due to their facile synthesis, structural flexibility, and high potential as efficient catalysts, numerous works have been carried out for the experimental and theoretical study of the oxo-peroxo-molybdenum(VI) complex of 4-furoyl-3-methyl-1-phenyl-pyrazolin-5-one. The main objective of this work is to determine the spectral properties of the title compound. Density functional theory (DFT) and ab initio methods were used extensively to calculate a variety of molecular properties such as molecular structure, molecular orbital, and vibrational spectrum.

Experimental

Material and methods

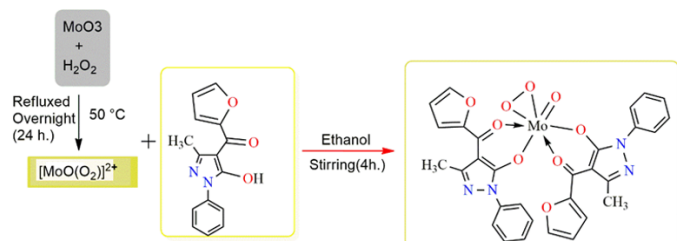
The chemicals used in this work were purchased commercially. Elemental analysis was determined by microanalysis at CDRI, Lucknow. The FTIR spectrum was recorded on a Bruker α T FT-IR spectrophotometer using potassium bromide pellets. The electronic spectrum was recorded using Varian Carry 5000, UV/Vis/NIR spectrophotometer. The electrochemical properties of the compound were determined with Epsilon BASi cyclic voltameter using TBAP as a supporting electrolyte. The decomposition temperature of the compounds was monitored using an electrically operated melting point apparatus with a heating capacity of up to 360°C. Theoretical studies, i.e., molecular geometric parameters and vibrational properties, frontier molecular orbitals (FMOs), and molecular electrostatic potential surfaces (MEPS) of the studied compound were performed using density functional theory (DFT) with B3LYP/LANL2DZ combinations. The DFT calculations were performed using the Gaussian 09 software package.

Preparation of complex

A white suspension of MoO_3 (0.025 M, 0.359 g) in 30% H_2O_2 (35 mL) was stirred for 24 hours at 50 °C giving a yellow solution was filtered and continuously added a solution of 4-furoyl-3-methyl-1-phenyl 2-pyrazoline-5-one (0.0025 M, 0.6702 g) in ethanol. The resulting solution was stirred for four hours and was allowed to cool in an ice bath. A lemon green precipitate appeared and was suction filtered with water-ethanol (1:1) solution and dried in a desiccator over anhydrous calcium chloride. Anal. calculated $\text{C}_{16}\text{H}_{18}\text{MoO}_2\text{N}_8/648.4$ C, 55.56; H, 3.73; N, 8.64 and Found C, 54.32; H, 3.61; N, 8.56, Yield 68 %, mp: 248, mc: 12.8 [$\Delta\text{M}(\Omega^{-1}\text{cm}^2\text{mole}^{-1})$] IR: $\nu(\text{C}=\text{O})$ 1666; $\nu(\text{C}=\text{N}_2)$ 1562, $\nu(\text{C}-\text{O})$ 1262, $\nu(\text{O}-\text{O})$ 820; $\nu(\text{Mo}=\text{O})$, 940; $\nu(\text{Mo}-\text{O})$ 762; and $\nu(\text{OH})$ 3411, UV-Vis. 251, 287, and 363 nm.

Results and discussion

The oxo-peroxo-molybdenum (VI) compound containing 4-furoyl-3-methyl-1-phenyl-pyrazoline-5-one under study was constructed according to the following Scheme 1.



Scheme 1 Synthetic route of oxoperoxomolybdenum(VI) complex.

Spectral studies

The essential experimental [theoretical] spectral bands and their tentative assignments of a title complex are discussed. The complex displays a strong band at 940 [960] cm^{-1} assigned to the $\nu(\text{Mo}=\text{O})$ mode. The metal peroxo grouping gives rise to three IR active vibrational modes, and these are (O-O) stretching (ν_1), symmetric (Mo-O) stretching (ν_2), and asymmetric (Mo-O) stretching (ν_3). The characteristic (ν_1) (O-O) mode of the complex appears at 820 [831] cm^{-1} , while the (ν_2) and (ν_3) modes appear at 680 [640] cm^{-1} and 754[803] cm^{-1} , respectively. These observations agree with results reported elsewhere.^{11,12} The experimental and theoretical FTIR spectrum are given in Figures 1 & 2, respectively.

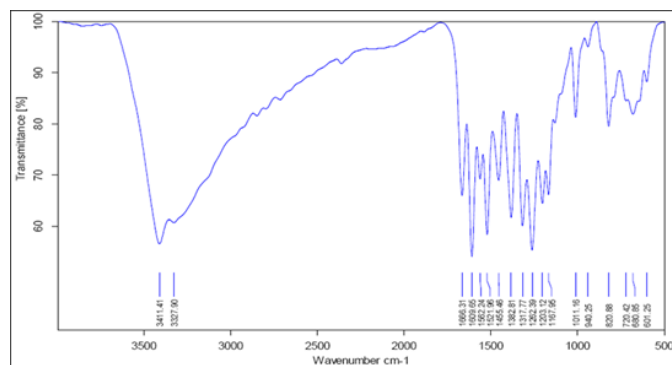


Figure 1 Experimental FT-IR spectrum of $[\text{MoO}(\text{O}_2)(\text{fmphp})_2]$.

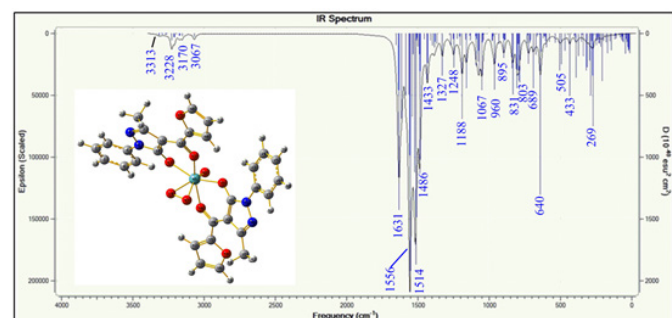


Figure 2 Theoretical I.R. spectrum of $[\text{MoO}(\text{O}_2)(\text{fmphp})_2]$.

The electronic spectrum of a complex was recorded in a 10^{-4} M DMSO solution. The high-intensity spectral peak in the complex UV region at 251 and 287 nm are due to intra-ligand transition.¹³ The low-intensity peak at 382 nm is assigned ligand to metal charge transfer transition. The respective spectrum has been shown in Figure 3.

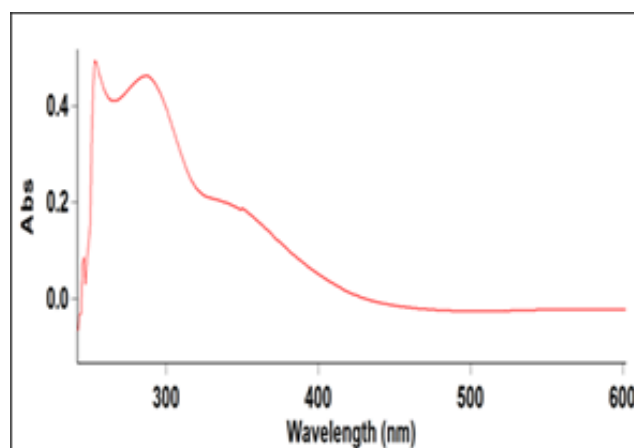


Figure 3 Electronic spectrum of $[\text{MoO}(\text{O}_2)(\text{fmphp})_2]$ in 10^{-4} DMSO solution.

The electrochemistry of the studied complex was monitored by cyclic voltammograms in DMSO with tetrabutylammonium perchlorate (TBAP) as a supporting electrolyte in the potential range ± 2000 mV versus current. It shows spectral and structural changes associated with electron transfer. The typical voltammograms are shown in Figure 4. The complex shows an irreversible redox wave as one-step electron reduction $\text{Mo(VI)}-\text{Mo(V)}$ and oxidation waves as one-electron oxidation $\text{Mo(V)}-\text{Mo(VI)}$. In these cases, the difference in peak potentials increases as the scan rate increases. The constancy of E_r shows that in all cases both peaks are complementary to each other. The peak current ratio I_{pa}/I_{pc} is less than one, indicating that the electron transfer reaction is followed by a chemical reaction EC mechanism.¹⁴

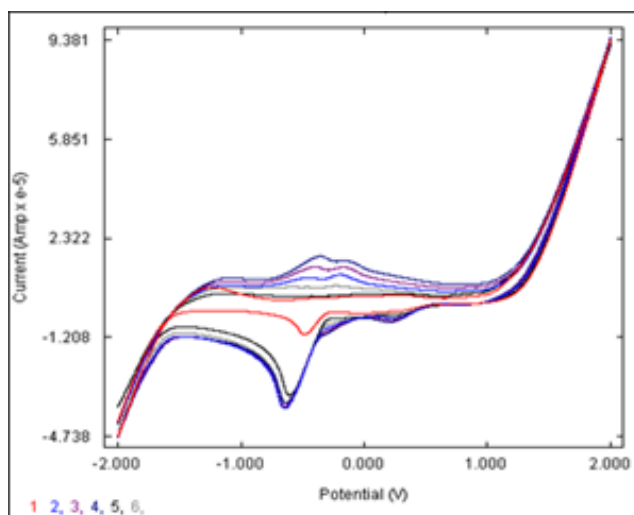


Figure 4 Cyclic voltammogram of $[\text{MoO}(\text{O}_2)(\text{fmphp})_2]$ in 0.05M TBAP [scan rate: 100, 200, 300, 400 and 500 (mV/s)].

Theoretical studies

The molecular structural parameter viz., bond lengths, and bond angles generated from the optimized structure of $[\text{MoO}(\text{O}_2)(\text{fmphp})_2]$ using Gaussian 09 software are given in Table 1. The optimized molecular structure is shown in Figure 5. The computed bond lengths, such as $\text{Mo}=\text{O}(48)$; 1.732(oxo), $\text{Mo}-\text{O}(14)$; 1.954 (peroxo), $\text{Mo}-\text{O}(45)2.114$ (peroxo), These results are comparable to the data reported elsewhere.¹⁵

Table 1 Selected geometrical parameter of complex, $[\text{MoO}(\text{O}_2)(\text{fmphp})_2]$

Bond connectivity	Bond length (Å)	Bond connectivity	Bond angle(°)	Bond connectivity	Bond angle(°)
O(14)-O(45)	1.4669	O(14)-Mo(46)-O(36)	124.13	O(36)-Mo(46)-O(48)	91.275
O(14)-Mo(46)	1.9542	O(14)-Mo(46)-O(45)	42.042	O(36)-Mo(46)-O(53)	82.642
O(36)-Mo(46)	2.0466	O(14)-Mo(46)-O(47)	74.666	O(36)-Mo(46)-O(54)	82.534
O(45)-Mo(46)	2.114	O(14)-Mo(46)-O(48)	134.618	Mo(46)-O(14)-O(45)	74.815
Mo(46)-O(47)	2.165	O(14)-Mo(46)-O(53)	100.725	Mo(46)-O(45)-O(14)	63.143
Mo(46)-O(48)	1.7324	O(14)-Mo(46)-O(54)	79.453	O(47)-Mo(46)-O(48)	81.69
Mo(46)-O(53)	2.0015	O(45)-Mo(46)-O(36)	82.156	O(47)-Mo(46)-O(53)	79.066
Mo(46)-O(54)	2.194	O(45)-Mo(46)-O(47)	114.238	O(47)-Mo(46)-O(54)	117.796
		O(45)-Mo(46)-O(48)	151.703	O(48)-Mo(46)-O(53)	112.124
		O(45)-Mo(46)-O(53)	94.382	O(48)-Mo(46)-O(54)	78.302
		O(45)-Mo(46)-O(54)	73.573	O(53)-Mo(46)-O(54)	162.036
		O(36)-Mo(46)-O(47)	156.163		

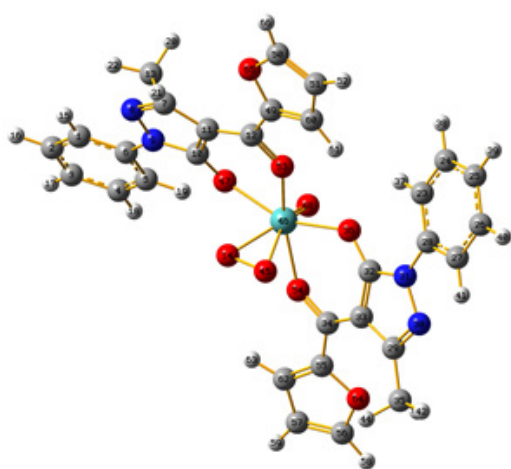


Figure 5 Optimized structure of the complex $[\text{MoO}(\text{O}_2)(\text{fmphp})_2]$.

The frontier molecular orbitals, i.e., the HOMOs and LUMOs, are crucial parameters for chemical reactions.¹⁶ They can be used to determine the mode of interaction between molecules and other species. Therefore, they are also referred to as boundary orbitals. The HOMOs act primarily as electron donors, while the LUMOs act primarily as electron acceptors. The gap between HOMO and LUMO characterizes molecular chemical stability.¹⁷ Here we have selected three pairs of six applicable molecular orbitals, namely the third highest [HOMO -2], the second highest [HOMO -1] and the highest occupied MO's [HOMO], the lowest [LUMO], the second lowest [LUMO+1] and the third lowest unoccupied MO's [LUMO+2] worked out for $[\text{MoO}(\text{O}_2)(\text{fmphp})_2]$. The observed energies in order are -6.457, -6.350, -6.270, -3.687, -3.220, and -2.682 eV, while the energy gap between [HOMO-LUMO], [HOMO -1-LUMO+1], and [HOMO -2-LUMO+2] is 2.584, 3.130, and 3.775 eV, respectively. The electronic filling scheme of FMOs for the complex molecule confirms that it is diamagnetic due to the paired electrons in HOMO. The chemistry of the softness and hardness of the molecule is based on the FMOs, the hard molecules have a higher value of the HOMO-LUMO gap and the soft molecules have a smaller value of the HOMO-LUMO gap.¹⁸ The LUMO is mainly localized at the donor and acceptor atoms around the metal. In comparison, HOMO is delocalized over the pyrazoline moiety. The HOMO-LUMO structures with an energy level audio diagram of the complex are shown in Figure 6. Another important property related to the dipole moment and hardness is the electrophilicity index (ω) and global softness (S), as indicated below. The values of ω and S are listed in Table 2.

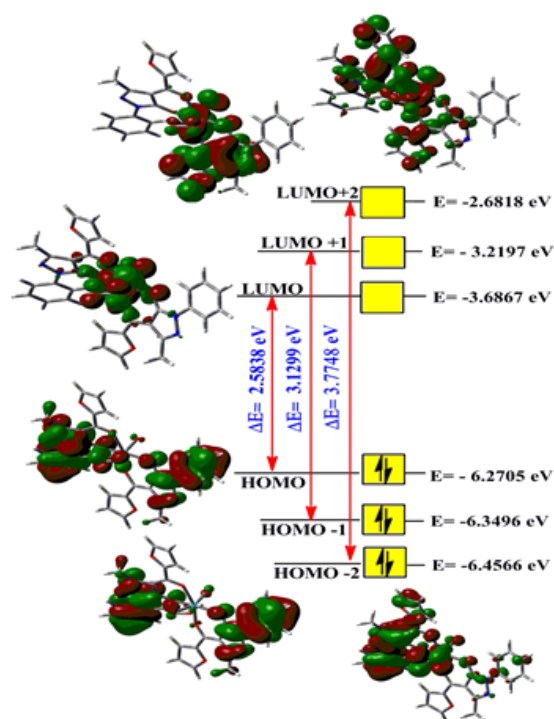


Figure 6 FMOs of $[\text{MoO}(\text{O}_2)(\text{fmphp})_2]$ with the energy in eV.

Table 2 Some theoretical data of the complex $[\text{MoO}(\text{O}_2)(\text{fmphp})_2] \cdot \text{H}_2\text{O}$ obtained by Gaussian 09 software

Parameters	I
Basis set	LANL2DZ
Charge	0
Spin	Singlet
Total energy	-57,680.5763
RMS gradient norm	0.0001475 eV
Imaginary freq	0
Dipole moment	2.9710 Debye
Point group	Cs
ΔE (HOMO-LUMO)	2.5838
Absolute hardness (η)	-1.2919
Absolute electronegativity (χ_{abs})	-4.9786
Electrophilicity index (ω)	-3.4162
Global softness (S)	-0.774

The MESP topology is used to understand the reactive actions, as negative regions can be considered nucleophilic centers. MESP-based characterization of a molecule in terms of electron-rich and electron-poor regions provides a meaningful prediction of its interaction with other molecules. In contrast, the positive regions are potential electrophilic centers. The surface of the molecular electrostatic potential¹⁹ is shown in Figure 7. It shows the molecular shape, size, and electrostatic potential values of the molybdenum(VI) complex. The MESP map of the studied compound shows that the carbonyl oxygen and hydroxyl oxygen atoms represent the most negative potential region. In contrast, the seven oxygen donor atoms are bound with the molybdenum center in the most negative region due to their nucleophilic tendency. The hydrogen atoms in the compound carry the region of maximum positive charge. The majority of the green regions in the MESP surfaces correspond to a potential halfway between the two extremes of the red and blue colors.

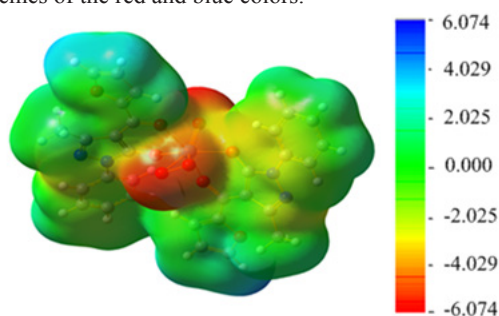


Figure 7 MEP of complex $[\text{MoO}(\text{O}_2)(\text{fmphp})_2]$.

Conclusion

The experimental-theoretical studies presented above suggest that the studied complex in question can be formulated as $[\text{MoO}(\text{O}_2)(\text{fmphp})_2]$, where fmphpH: 4-furoyl-3-methyl-1-phenyl-pyrazolin-5-one. Considering the combinatorial experimental and calculated data, a suitable hepta-coordinated distorted pseudo-pentagonal bipyramidal geometry was proposed for the study complex, as shown in Figure 5. Based on the experimental and theoretical results, the assignments of the fundamental frequencies were observed. The computational HOMO and LUMO energies show that charge transfer occurs within the molecules.

Acknowledgments

The authors are thankful to our Vice-Chancellor Prof. Kapil Deo Mishra and Head for encouragement. Analytical facilities provided by the Central Drug Research Institute, Lucknow, India.

Funding

None.

Conflicts of interest

There is no conflict of interest.

References

1. Jensen BS. The synthesis of 1-phenyl-3-methyl-4-acyl-pyrazolones-5. *Acta Chem Scand.* 1959;13:1668–1670.
2. Maurya RC, Sutradhar D, Martin MH, et al. Oxovanadium(IV) complexes of medicinal relevance: Synthesis, characterization and 3Dmolecular modeling and analysis of some oxovanadium(IV) complexes in O, N-donor coordination matrix of sulfa drug Schiff bases derived from a 2-pyrazoline-5-one derivative. *Arabian Journal of Chemistry.* 2015;8:78–92.
3. Marchetti F, Pettinari C, Pettinari R. Acylpyrazolone ligands: Synthesis, structures, metal coordination chemistry and applications. *Coord Chem Rev.* 2005;249:2909–2945.
4. Goodman LS, Gilman A. The pharmacological basis of therapeutics, fourth ed. McMillan and Co., London; 1970.
5. Garg HG, Singh PP. Potential antidiabetics. VI. 3-Methyl-4-arylhydrazono-2-isoxazolin-5-ones and 3-methyl-4-aryloxy-5-(methyl phenyl)isoxazoles. *J Med Chem.* 1970;13(6):1250–1251.
6. Hille R, Hall J, Basu P. The mononuclear molybdenum enzymes. *Chem Rev.* 2014;114:3963–4038.
7. Pritsos CA, Gustafson DL. Xanthine dehydrogenase and its role in cancer chemotherapy. *Oncol Res.* 1994; 6(10–11): 477–481.
8. Haywood S, Dincer Z, Holding J, et al. Metal (molybdenum, copper) accumulation and retention in brain, pituitary and other organs of ammonium tetrathiomolybdate-treated sheep. *Br J Nutr.*1998;79:329–331.
9. Thompson KH, McNeill JH, Orvig C. Vanadium compounds as insulin mimics. *Chem Rev.* 1999;99:2561–2572.
10. Waern JB, Harding MM. Bio organometallic chemistry of molybdocene dichloride. *J Organomet Chem.* 2004;689:4655–4668.
11. Mir JM, Maurya RC, Vishwakarma PK. Corrosion resistance and thermal behavior of acetylacetonato-oxoperoxomolybdenum(VI) complex of maltol: Experimental and DFT studies. *Karbala International Journal of Modern Science.* 2017;3:212–223.
12. Maurya RC, Bohre P, Sahu S, et al. Oxoperoxomolybdenum(VI) complexes of catalytic and biomedical relevance: Synthesis, characterization, antibacterial activity and 3D-molecular modeling of some oxoperoxomolybdenum(VI) chelates in mixed(O,O) coordination environment involving maltol and b-diketoenolates. *Arabian Journal of Chemistry.* 2016;9:150–160.
13. Litos C, Terzis A, Raptopoulou C, et al. A. Polynuclear oxomolybdenum(VI) complexes of dihydroxybenzoic acids: Synthesis, spectroscopic and structure characterization of a tetranuclear catecholato-type coordinated 2,3-dihydroxybenzoate and a novel tridentate salicylato-type coordinated 2,5-dihydroxybenzoate trinuclear complex. *Polyhedron.* 2006;25:1337–1347.
14. Patel RN, Gundla VLN, Patel DK. Synthesis, structure and properties of some copper(II) complexes containing an ONO donor Schiff base and substituted imidazole ligands. *Polyhedron.* 2008;27:1054–1060.
15. Saheb V, Sheikhshoaie I, Stoeckli-Evans H. A novel tridentate Schiff base dioxo-molybdenum(VI) complex: Synthesis, experimental and theoretical studies on its crystal structure, FTIR, UV-visible, ¹H NMR and ¹³C NMR spectra. *Spectrochim Acta A.* 2012;95:29–36.
16. Shoba D, Periandy S, Karabacak M, et al. Vibrational spectroscopy (FT-IR and FT-Raman) investigation and hybrid computational (HF and DFT) analysis on the structure of 2,3-naphthalenediol. *Spectrochim Acta A.* 2012;83:540–552.
17. Fukui K. Role of frontier orbitals in chemical reactions. *Science.* 1982;218:747–754.
18. Pearson RG. The principle of maximum hardness. *Accounts of Chemical Research.* 1993;26(5):250–255.
19. Mir JM, Vishwakarma PK, Malik BA, et al. An old oxovanadium(IV) complex of N-(salicylidene)sulfanilamide: theoretical validity of experimental observations. *Inorganic and Nano-Metal Chemistry.* 2019;48(8):1–9.